LAWRENCE
LIVERMORE
NATIONAL
LABORATORY

LLNL-JRNL-430953

Instrumentation of spin resolved photoelectron spectroscopy and bremsstrahlung isochromat spectroscopy

S. W. Yu, B. W. Chung, G. D. Waddill, J. G. Tobin

May 10, 2010

Review of Scientific Instruments

Disclaimer

Instrumentation of spin resolved photoelectron spectroscopy and bremsstrahlung isochromat spectroscopy

S.-W. Yu,[1,*] B. W. Chung,[1] G. D. Waddill,[2] and J. G. Tobin[1]

[1]*Lawrence Livermore National Laboratory, Livermore, CA*

[2]*Missouri University of Science and Technology, Physics Department, Rolla, MO*

Abstract

We have built a new system for spin resolved photoelectron spectroscopy and bremsstrahlung isochromat spectroscopy at the Lawrence Livermore National Laboratory to investigate the electronic structures of the actinides, which are very toxic and radioactive materials, and therefore cannot be brought to general user facilities for spectroscopic researches. We describe the technical details for the new system and provide the preliminary data obtained from the new system.

PACS numbers:

*Corresponding Author: YU21@LLNL.GOV

I. INTRODUCTION

Actinides science, which is the study of the elements with atomic numbers in the range 90 and 103, has received a great attention recently due to their important roles in the threat of nuclear terrorism and the use of nuclear power and the safer management of the nuclear waste [1]. In addition to the well-known nuclear reactions of these heavy radioactive actinides, the $5f$ electrons in the valence shell yield fascinating physical and chemical properties, which are all revealing signs of the correlations among $5f$ electrons, resulting in behavior that cannot be explained by the one-electron band theory [2]. For example, right at plutonium (Z=94) the $5f$ electrons makes an abrupt transition between from being itinerant to being localized. Consequently, plutonium is notoriously unstable with temperature, pressure, chemical additions, and time. Continuous efforts are essential to understand the nature of the $5f$ electron correlations [1–10].

One of the most powerful tools to study the electron correlations is the electron spectroscopies, e.g. (high resolution and spin resolved) photoelectron spectroscopy for the occupied states [2–10] and bremsstrahlung isochromat spectroscopy (inverse photoemission spectroscopy at high energy) for the unoccupied states [11, 12], and also x-ray absorption spectroscopy, requiring the use of the synchrotron radiation. From experimental point of view, however, the most challenging obstacle is that due to the toxicity and the radioactivity of the actinides, it is extremely difficult to bring the actinides samples to the synchrotron radiation facilities for these spectroscopic studies. In order to overcome this difficult, a spectroscopic system containing high resolution and spin resolved photoelectron spectroscopy and bremsstrahlung isochromat spectroscopy has been built at the Lawrence Livermore National Laboratory (LLNL), utilizing the special sample handling system for the actinides experienced at the LLNL. Therefore, the aim of this paper is to report on the design and performance of the new system, and to present the preliminary results.

The structure of this article is as follows. In sections II and III, we provide an overview and technical details for spin resolved photoelectron spectroscopy and bremsstrahlung isochromat spectroscopy. In section IV, we provide the preliminary data obtained with the new system.

II. OVERVIEW OF THE NEW SYSTEM

Fig. 1 illustrates an overview of the new system for high resolution and spin resolved photoelectron spectroscopy (PES) and bremsstrahlung isochromat spectroscopy (BIS). For PES, as the photon sources, there are two unpolarized ultraviolet lights (UV1 and UV2) located in X-Z plane and an unpolarized x-ray source located in Y-Z plane. The advantage of the two UV sources is that the instrumental asymmetries, which is very crucial in the spin resolved photoelectron spectroscopy, can be eliminated with the two UV sources [13]. The energies of the photoelectrons are analyzed by the hemispherical electron energy analyzer by means of 6 channels MCD (Multichannel Detector) located at the exit plane of the analyzer (high resolution PES). The electrons in central part of the exit plane are fed through the 7 mm diameter aperture into the acceleration lens in which electrons are accelerated for their spin analysis in the Mott detector [14–19].

For BIS, a monochromatic electron beam hits the sample. The bremsstrahlung emitted in the energy range of 20-1500 eV is measured by BIS spectrometer, which is designed under Rowland circle geometry [20] and consists of an entrance slit, two moveable shutters for grating selection, three spherical gratings, and a two dimensional detector that can be translated along the X- and Y-directions and rotated around the Z-axis to follow the path of the Rowland circle.

In addition, there is a sample preparation chamber, which is connected to a special exhaust line and can be isolated physically from the main chamber. Actinide samples can be prepared in this preparation chamber before spectroscopic studies.

III. TECHNICAL DETAILS

A. Energy and spin resolved photoelectron spectroscopy

A commercially available hemispherical electrostatic electron energy analyzer combined with Mott detector (PHOIBOS 150 from SPECS, Inc) has been used to analyze the energy and the spin of the photoelectrons. Figure 2 show a sketch for the main analyzer components including Mott detector. The main components are: lens system for receiving charged particles, 180° hemispherical analyzer for performing spectroscopic energy measurements, detector assembly for nonspin particle detection, and Mott detector. The input lens system

define the analysis area and angular acceptance by imaging the emitted electrons onto the entrance slit of the analyzer. Particles passing through the lens are focused onto the entrance slit S1. The hemispherical analyzer with a mean radius (r_0=150 mm) measures the energy of the photoelectrons. The photoelectrons entering the hemispherical analyzer through the entrance slit S1 are deflected into elliptical trajectories by the radial electrical field between the inner hemisphere (r_{in}=0.75r_0) and the outer hemisphere (r_{out}=1.25r_0). The entrance slit S1 and exit plane S2, are centered on the mean radius r_0. For a fixed electrical field gradient, only electrons with kinetic energies in a certain energy interval are able to pass through the full deflection angle from the entrance slit S1 to the exit plane S2. Electrons on the central trajectory possess the nominal pass energy. They are focused to the central radial position at the exit plane S2. Electrons with higher kinetic energy are focused further outside, and electrons with lower kinetic energy are focused further inside in the exit plane S2. This offers the possibility of multichannel detection, with simultaneously recording of an energy band around the nominal pass energy. The electrons at the exit plane S2 of the analyzer are detected with 6 standard channeltrons in the nonspin detector assembly. Each channeltron has an opening of 7x20 mm. The electrons in the central part of the exit plane are directed through a 7 mm diameter aperture into the acceleration lens. The electrons accelerated through the acceleration lens hit a Thorium target at 25 kV. After the electrons are scattered from this target, they are detected by 4 channeltrons in the Mott detector, in which two transversal spin components P_X and P_Y are determined simultaneously (spin resolved PES) [14–19].

B. Bremsstrahlung Isochromat Spectroscopy

Our BIS spectrometer is composed of a soft x-ray emission spectrometer (a commercial available XES 350 system from VG Scienta Ltd) and an electron gun, which can provide electrons with energies of 20-5000 eV. The excitation current at the sample depends on the energy, but typically, 10 μA at 3 keV and 3 μA at 900 eV [21]. The base pressure of the system was 3 x 10^{-10} torr, but the pressure changed depending on the energy of the electron. For example, the pressure was approximately 8 x 10^{-10} torr at 3 keV. The optical arrangement of the XES 350 system follows Rowland circle geometry [20] and its main components are: an entrance slit, three spherical gratings, and a detector. The Rowland

circle geometry expresses the fact that diffracted photons of all the wavelengths will be focused on the circumference of a circle of radius R, which is known as the Rowland circle, if the entrance slit are located on the circle and the grating with curvature of radius $2R$ is placed tangentially to the circle, as shown in Fig. 3. Photons of different wavelengths are diffracted according to the grating equation

$$n\lambda = d(\sin\alpha + \cos\beta), \tag{1}$$

where the integer n stands for different orders of diffraction, d is the distance between two grooves, α and β are the angles for incident and diffracted photons, respectively. Since XES 350 has three spherical gratings, a common entrance slit, and a common detector, in conceptually, XES 350 system can be seen as three different Roland spectrometers combined into a single spectrometer to have a common entrance slit and a common detector that can be aligned to the Roland circle of the grating in use.

The entrance slits is made of two blades fixed in respective to each other, but with a ability to rotate around an axis parallel to the slit edges and located in the center of the assembly. The projected slit size seen by gratings can be varied continuously from 100μm down to a completely closed slit, which allows us to change the spectral resolution. Selection of grating is carried out by means of two shutters forming an aperture, which defines the illuminations of the grating selected. Table 1 shows the parameters for the three gratings.

Grating	Radius	Groove density	Grazing angle	Operating range
1	5 m	1200 l/mm	1.9°	≈300-1500 eV
2	5 m	400 l/mm	2.6°	≈100-450 eV
3	3 m	300 l/mm	5.4°	≈20-200 eV

TABLE I: Grating parameters

IV. SYSTEM PERFORMANCES

A. Spin resolved photoelectron spectroscopy

We present spin resolved core level $2p_{1/2}$ photoelectron spectra of Cu(100) single crystal with unpolarized light of hν=1253.6 eV for the two spin components P_X and P_Y, as shown in

Fig. 4. For the determination of the spin component P_X, the following equation is used [13]

$$P_X = \frac{1}{S_{\text{eff}}}\left(\frac{A_X - A_X^0}{1 - A_X A_X^0}\right), \tag{2}$$

where S_{eff} is the Sherman function ($S_{\text{eff}} = 0.16 \pm 0.04$) and A_X is the asymmetry given by$A_X = \frac{N_1 - N_2}{N_1 + N_2}$, with N_1 and N_2 of the numbers of electrons scattered to the counter 1 and counter 2, respectively, in the Mott detector shown in Fig. 1. The instrumental asymmetry A_X^0 is assumed as a line and shown as red line in the bottom panel of Fig. 4(a). The determined spin component P_X is given in the middle panel of Fig. 4(a). The spin integrated total intensity I is separated into the partial intensities for spin parallel I_+ and antiparallel I_- to X-direction, by means of $I_\pm = (I/2)(1 \pm P_X)$. I and $I_\pm$ are shown in the top panel of Fig. 4(a). Similarly, the spin component P_Y is determined as shown in Fig. 4(b).

As shown in Fig. 4, we clearly observe nonzero spin polarization along the X-direction (P_X), but zero spin polarization along the Y-direction (P_Y). The reason is as follows. Under our experimental geometry given Fig. 1, the x-ray tube is located in the Y-Z plane. The X-direction is perpendicular to the reaction plane defined by the incident photons and the outgoing electrons while the Y-direction is parallel to the reaction. Based on the parity conservation law for the electromagnetic interaction, which governs electron scattering [15], the spin component P_X, which is perpendicular to the reaction plane, obeys the parity conservation law and can retain its direction. But the spin component P_Y, which is parallel to the reaction, violates the parity conservation law and cannot retain its direction. In general, due to the parity conservation law, a nonzero spin component in photoelectron experiment with unpolarized light is expected only if the spin component is perpendicular to the reaction plane.

B. X-ray emission spectroscopy and bremsstrahlung isochromat spectroscopy

When a high energy electron beam impinges on a material, many events can happen as shown schematically in Fig. 5. First of all, some electrons just change their direction due to the nuclear in the material and emit the background bremsstrahlung. Some other electrons create core holes, which can be annihilated by other core electrons, with characteristic x-ray emission (x-ray emission spectroscopy). Other possibility is that a few electrons of the incident electron beam are decelerated into the unoccupied states of the material with a

spontaneous emission of bremsstrahlung. This bremsstrahlung process can be considered as the inverse of the photoemission process if the initial and final states are exchanged and the occupied state is replaced by the unoccupied one. BIS (Bremsstrahlung Isochromat Spectroscopy) is a very powerful tool to study the bulk unoccupied electronic structures of materials, minimizing the impact of surface effects. Due to the very low cross section for BIS, the BIS signal is extremely low compared to the one of x-ray emission.

In Fig. 6, we present 2p x-ray emission spectrum of Cu(100) single crystal with an electron energy of E=3 keV. The emission lines L$\alpha_{1,2}$ ($2p_{3/2}$) and Lβ_1 ($2p_{1/2}$) are observed at the emission energies of 930 eV and 950 eV, respectively. Since the intensities of the emission lines L$\alpha_{1,2}$ and Lβ_1 are very strong, the background bremsstrahlung is relatively reduced. The upper panel of Fig. 6 shows the corresponding detector image.

For BIS, we present the BIS spectra from UO_2 measured with three different electron energies of 720 eV, 815 eV, and 915 eV, as shown in Fig. 7. Because a BIS spectrum is an emission created by the deceleration of the incident electrons into the unoccupied states, the emission energy of a BIS epectrum should be proportional to the energy of the incident electron beam, as demonstrated in Fig. 7.

A combination of a XPS with hν=1486 eV and a BIS with E=736 eV is exhibited in Fig. 8. Since XPS and BIS spectra represent the occupied and unoccupied valence bands, respectively, the combination of XPS and BIS spectra is a powerful tool to investigate both the occupied and the unoccupied electronic structures of the actinides.

C. Resonant inverse photoelectron spectroscopy

Resonance in photoelectron spectroscopy, which is originated from the quantum mechanical interference of a direct transition to a continuum state, and a indirect transition involving a core level, is well known phenomena [22]. The interference between the two channels leads to an enhancement of the photoelectron cross section. Based on the atomic character of the core level and dipole selection rules, only appropriate symmetries of valence states are enhanced. Therefore, resonance photoelectron spectroscopy (RPES) provides local and symmetry-selective information on the systems under study [23].

By analogy with RPES, resonance behavior can be identified in the inverse photoelectron spectroscopy (IPES) [24–28]. Resonance inverse photoelectron spectroscopy (RIPES) can be

described in the following way. As shown schematically in Fig. 9, an incoming electron is decelerated into the partially unoccupied state with a spontaneous emission of bremsstrahlung (direct channel). When the energy of the incoming electron is equal to the binding energy of a core electron, the identical final state can be reached via a different path involving an intermediate state with a core hole (indirect channel). Then, the direct and the indirect channels interfere coherently, and lead an enhancement of the inverse photoelectron cross section. For example, for a ground state with N electrons in the partially occupied f shell, the direct channel is

$$|d^{10}f^{N}\rangle + e^{-} \rightarrow |d^{10}f^{N+1}\rangle + h\nu, \tag{3}$$

and the corresponding indirect channel is

$$|d^{10}f^{N}\rangle + e^{-} \rightarrow |d^{9}f^{N+2}\rangle \rightarrow |d^{10}f^{N+1}\rangle + h\nu. \tag{4}$$

Here, a core hole in d core level is created and filled by a f electron with the emission of bremsstrahlung. Since the initial and the final states of the both channels are identical, they can give rise to the resonant enhancement in the inverse photoemission.

As an example for RIPES, we present RIPES spectra from cerium-oxide as shown in Fig. 10. First of all, XES from Ce 3d with E= 3keV is shown in the middle of Fig. 10. When the BIS spectra are measured by changing the energies of the incident electron around the threshold of $3d_{5/2}$, the BIS intensity is enhanced resonantly as a result of coherent interference between direct and indirect channels, as shown in the left side of Fig. 10. In this case, the core hole at the Ce $3d_{5/2}$ is involved as the intermediate state. The similar resonant behavior is observed at the $3d_{3/2}$, as shown in the right side of Fig. 10.

V. CONCLUSIONS

We have built a spectroscopic system of spin resolved photoelectron spectroscopy and bremsstrahlung isochromat spectroscopy to investigate the electronic structures of the actinides at the LLNL. The new system is fully operational. We have presented the spin resolved photoelectron spectra from Cu 2p excited with unpolarized x-ray of hν=1253.6 eV and the x-ray emission spectrum from the Cu 2p excited with electron beam of E=3 keV. We have also provided the BIS spectra and a combination of XPS and BIS spectra from

UO_2. Finally, we have presented RIPES spectra from cerium-oxide. This new system will be used for the actinides researches, especially for Pu.

VI. ACKNOWLEDGMENTS

Lawrence Livermore National Laboratory is operated by Lawrence Livermore National Security, LLC, for the U.S. Department of Energy, National Nuclear Security Administration under Contract DE-AC52-07NA27344. This work was supported by the DOE Office of Science, Office of Basic Energy Science, Division of Materials Science and Engineering.

---

[1] S. S. Hecker, D. R. Harbur, and T. G. Zocco, Progress in Materials Science **49**, 429 (2004).

[2] K. T. Moore and G. van der Laan, Review of Modern Physics **81**, 235(2009).

[3] J. G. Tobin, B. W. Chung, R. K. Schulze, J. Terry, J. D. Farr, D. K. Shuh, K. Heinzelman, E. Rotenberg, G. D. Waddill, and G. van der Laan, Phys. Rev. B **68**, 155109 (2003).

[4] J. G. Tobin, K. T. Moore, B. W. Chung, M. A. Wall, A. J. Schwartz, G. van der Laan, and A. L. Kutepov, Phys. Rev. B **72**, 085109 (2005).

[5] S.-W. Yu, T. Komesu, B. W. Chung, G. D. Waddill, S. A. Morton, and J. G. Tobin, Phys. Rev. B **73**, 075116 (2006).

[6] J. G. Tobin, S. W. Yu, T. Komesu, B. W. Chung, S. A. Morton, and G. D. Waddill, Europhys. Lett. **77**, 17004 (2007).

[7] S. W. Yu, J. G. Tobin, and P. Söderlind, J. Phys.: Condens. Matter **20**, 422202 (2008).

[8] J. H. Shim, K. Haule, and G. Kotliar, Nature **446**, 513 (2007).

[9] J. H. Shim, K. Haule, S. Savrasov, and G. Kotliar, Phys. Rev. Lett. **101**, 126403 (2008).

[10] C. A. Marianetti, K. Haule, G. Kotliar, and M. J. Fluss, Phys. Rev. Lett. **101**, 056403 (2008).

[11] J. K. Lang and Y. Baer, Rev. Sci. Instrum. **50(2)**, 221 (1979).

[12] E. Wuilloud, H. R. Moser, W.-D. Schneider, and Y. Baer, Phys. Rev. B **28**, 7354 (1983).

[13] S.-W. Yu, B. W. Chung, J. G. Tobin, Takashi Komesu, and G. D. Waddill, Nuclear Instruments and Methods in Physics Research A, **614**, 145 (2010).

[14] N. F. Mott, H. S. W. Massey, *The Theory of Atomic Collisions* (Clarendon Press, Oxford, 1965).

[15] J. Kessler, *Polarized Electrons*, 2nd ed. (Spring-Verlag, Berlin, 1985).

[16] D. M. Oro, W. H. Butler, F. C. Tang, G. K. Walters, and F. B. Dunning, Rev. Sci. Instrum. 62, 667 (1991).

[17] F.B. Dunning, Nucl. Instr. and Meth. in Phys. Res. A **347**, 152 (1994).

[18] G. C. Burnett, T. J. Monroe, and F. B. Dunning, Rev. Sci. Instrum. 65(6), 1893 (1994).

[19] G. Ghiringhelli, K. Larsson, and N. B. Brookes, Rev. Sci. Instrum. 70, 4225 (1999).

[20] J. A. R. Samson, *Technique of Vacuum Ultraviolet spectroscopy*, Wiley, 1967.

[21] J. G. Tobin, S. W. Yu, B. W. Chung, G. D. Waddill, E. Damian, L. Duda, and J. Nordgren, submitted to PRB (2010).

[22] U. Fano, Phys. Rev. **124**, 1866 (1961).

[23] J. P. Connerade, J. M. Esteva, and R. C. Karnatak, *Giant Resonances in Atoms, Molecules, and Solids*, Plenum Press, New York, 1987.

[24] P. Weibel, M. Grioni, D. Malterre, B. Dardel, and Y. Baer, Phys. Rev. Lett. **72**, 1252 (1994).

[25] M. Grioni, P. Weibel, D. Malterre, and Y. Baer, Phys. Rev. B **55**, 2056 (1997).

[26] M. Grioni, P. Weibel, M. Hengsberger, and Y. Baer, J. Electron Spectrosc. Relat. Phenom **101-103**, 713 (1998).

[27] K. Kanai, Y. Tezuka, T. Terashima, Y. Muro, M. Ishikawa, T. Uozumi, A. Kotani, G. Schmerber, J. P. Kappler, J. C. Parlebas, and Shin, Phys. Rev. B **60**, 5244 (1999).

[28] K. Kanai, T. Terashima, A. Kotani, T. Uozumi, G. Schmerber, J. P. Kappler, J. C. Parlebas, and Shin, Phys. Rev. B **63**, 033106 (2001).

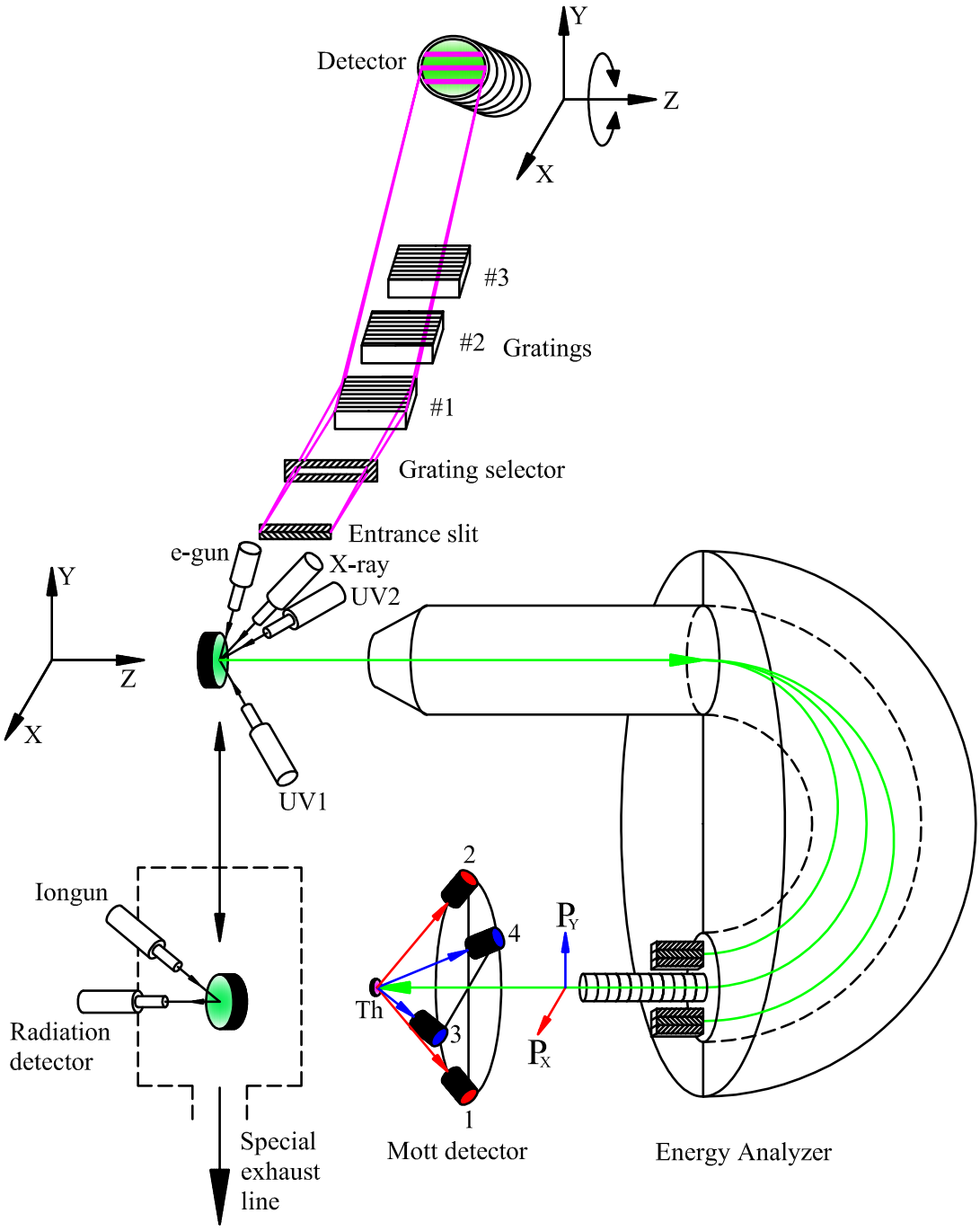

FIG. 1: (Color online) Sketch for the spin resolved photoelectron spectroscopy (SRPES) and Bremsstrahlung Isochromat Spectroscopy(BIS) installed recently at the Lawrence Livermore National Lab to study the electronic structures of the actinides.

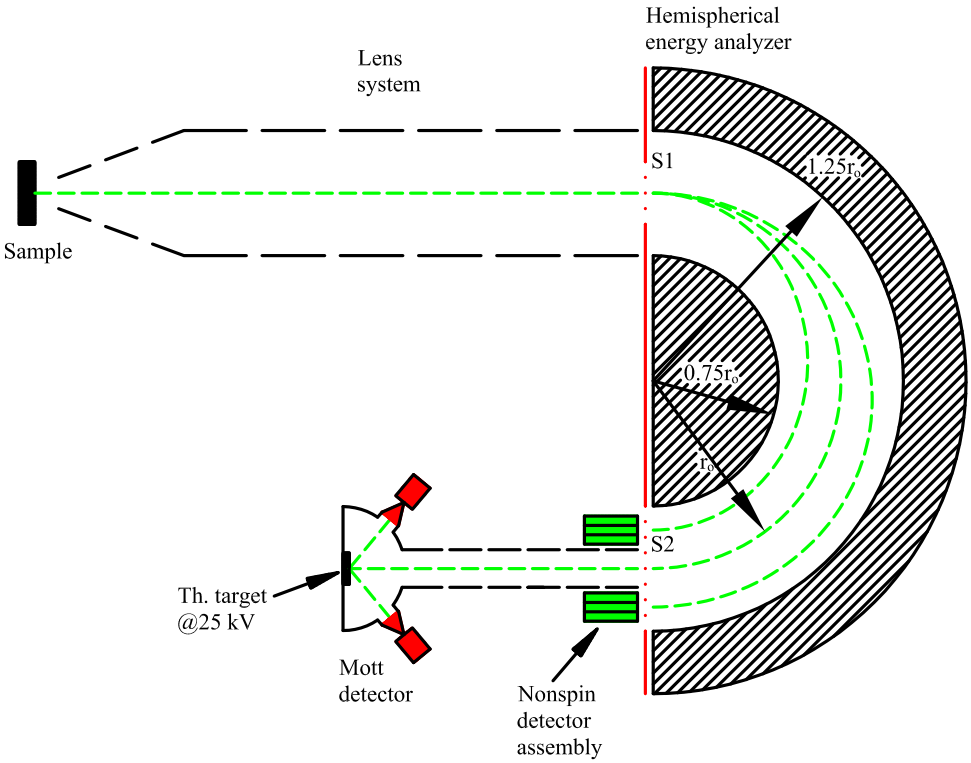

FIG. 2: (Color online) Sketch for analyzer main components: Lens system, hemispherical energy analyzer, nonspin detector assembly, and Mott detector for spin analysis.

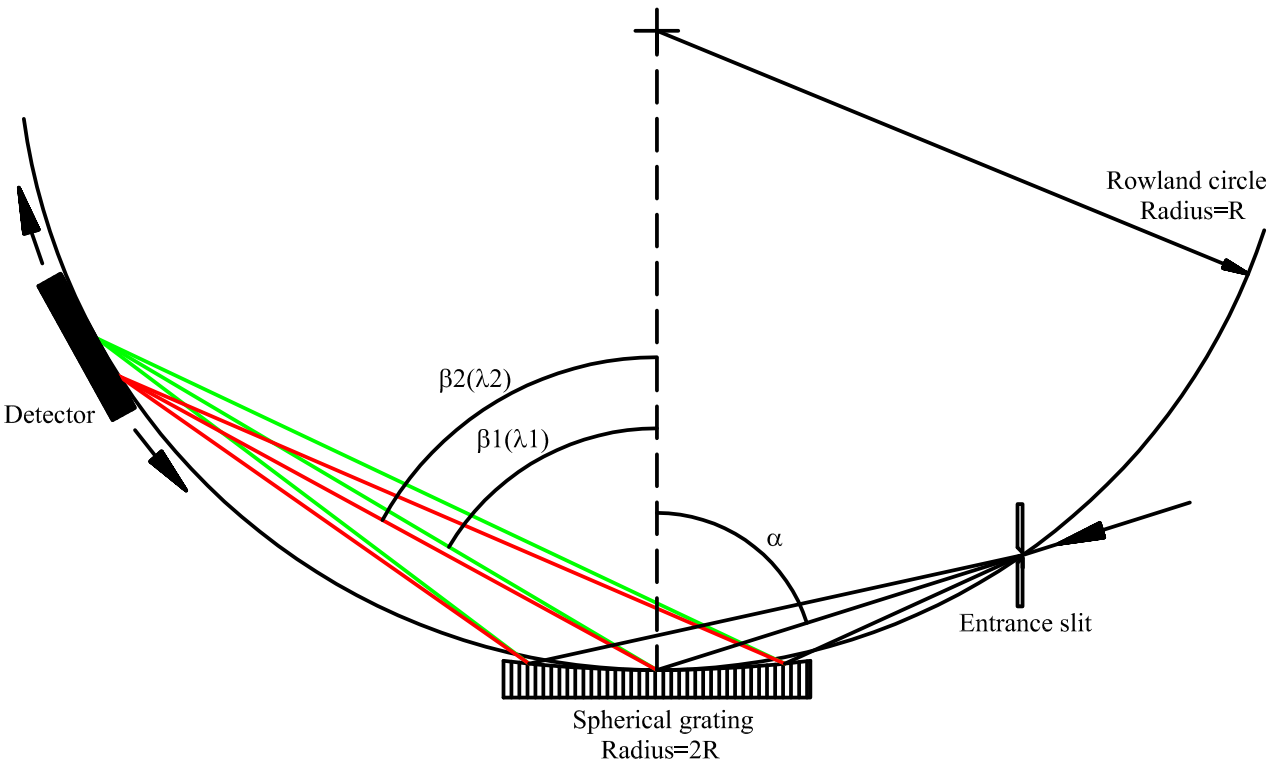

FIG. 3: (Color online) Rowland circle geometry of BIS system. The entrance slit, the grating, and the detector are on the Rowland circle of radius R.

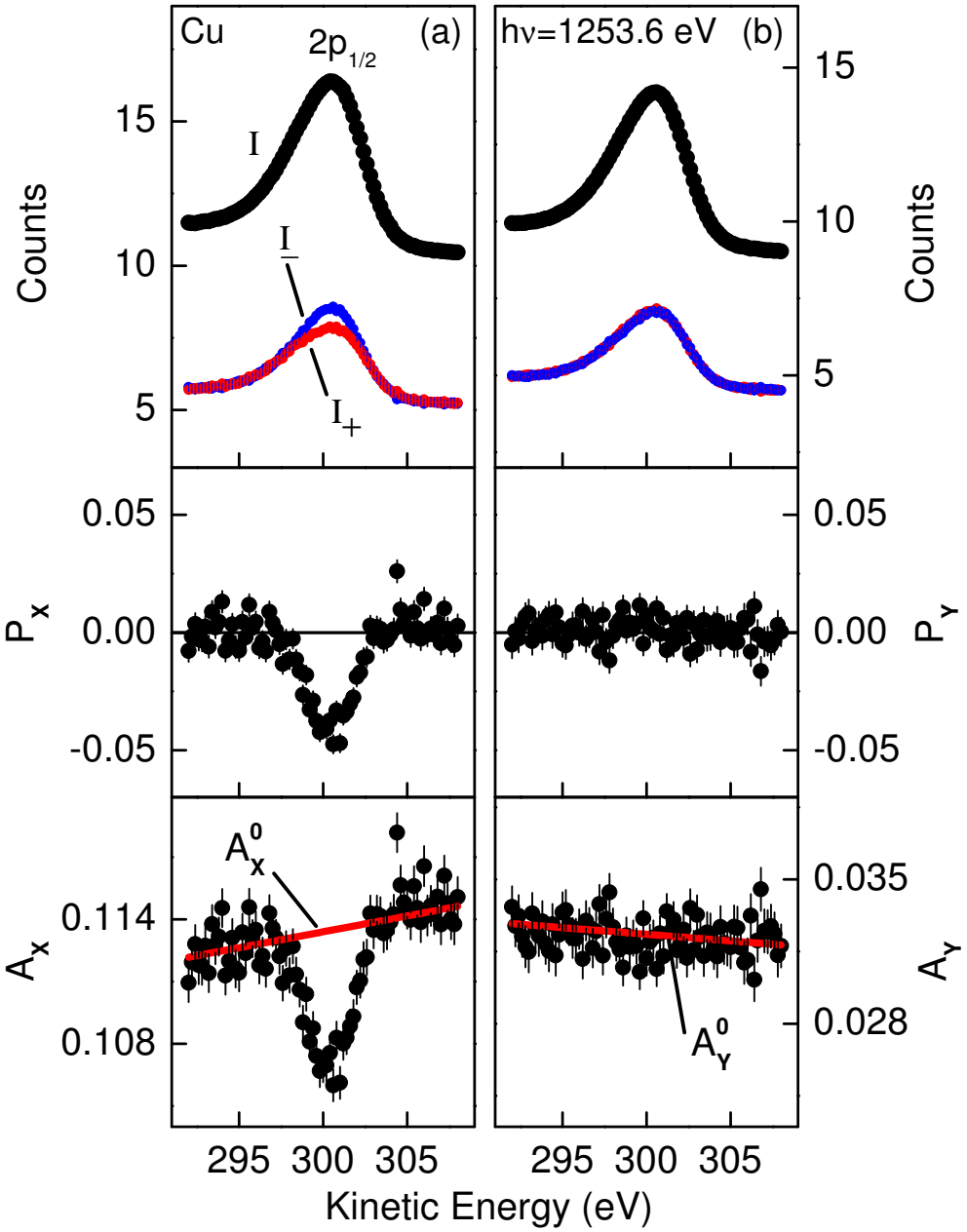

FIG. 4: (Color online) Spin resolved $2p_{1/2}$ core level photoelectron spectra of Cu(100) single crystal with unpolarized light of hν=1253.6 eV for the two spin components P_X in (a) and P_Y in (b).

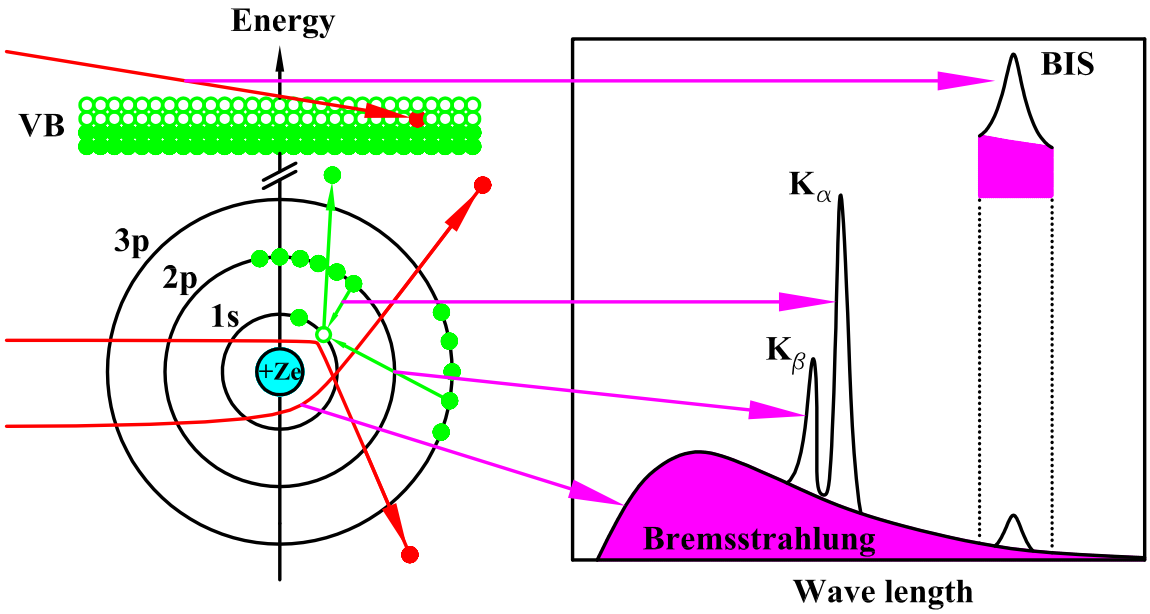

FIG. 5: (Color online) Sketch for a generation of background bremsstrahlung, XES, and BIS with a high energy electron beam.

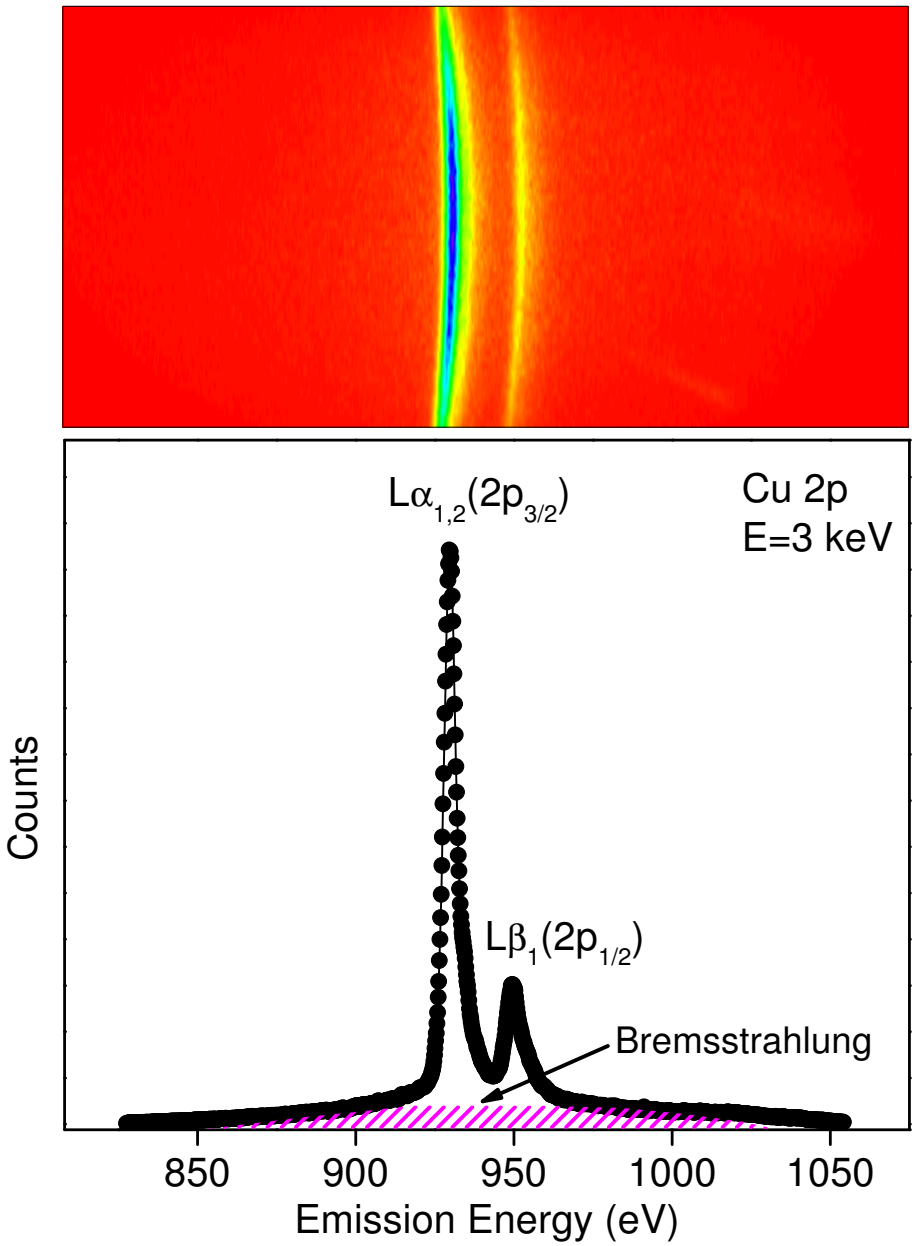

FIG. 6: (Color online) L$\alpha_{1,2}$ ($2p_{3/2}$) and Lβ_1 ($2p_{1/2}$) x-ray emission spectra from Cu with an electron energy of E=3 keV. The top part shows the corresponding detector image.

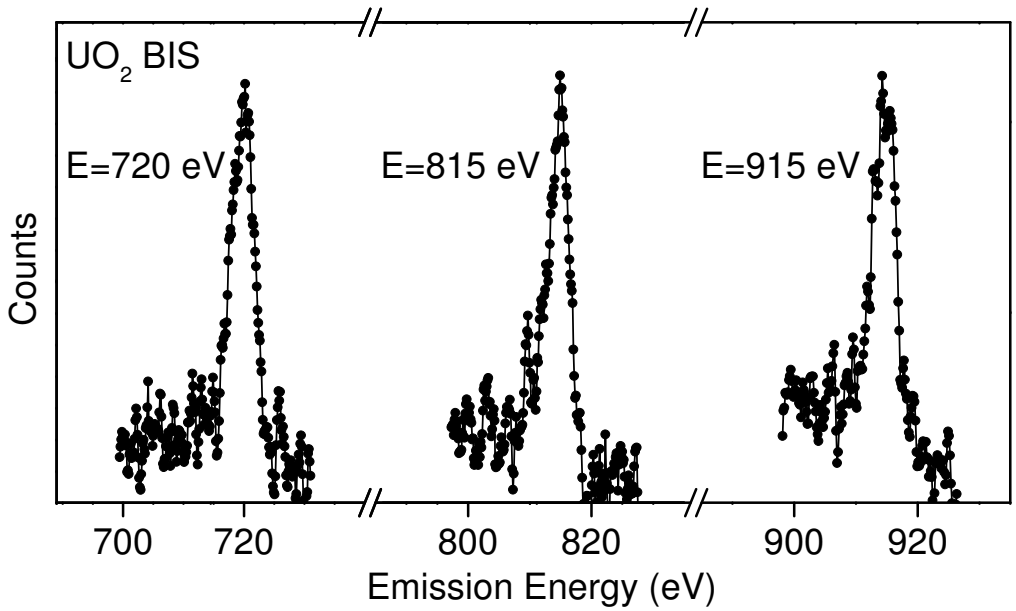

FIG. 7: (Color online) BIS spectra from UO2 with three different electron energies of E=720 eV, 815 eV, and 915 eV. The emission energy is proportional to the incident electron energy.

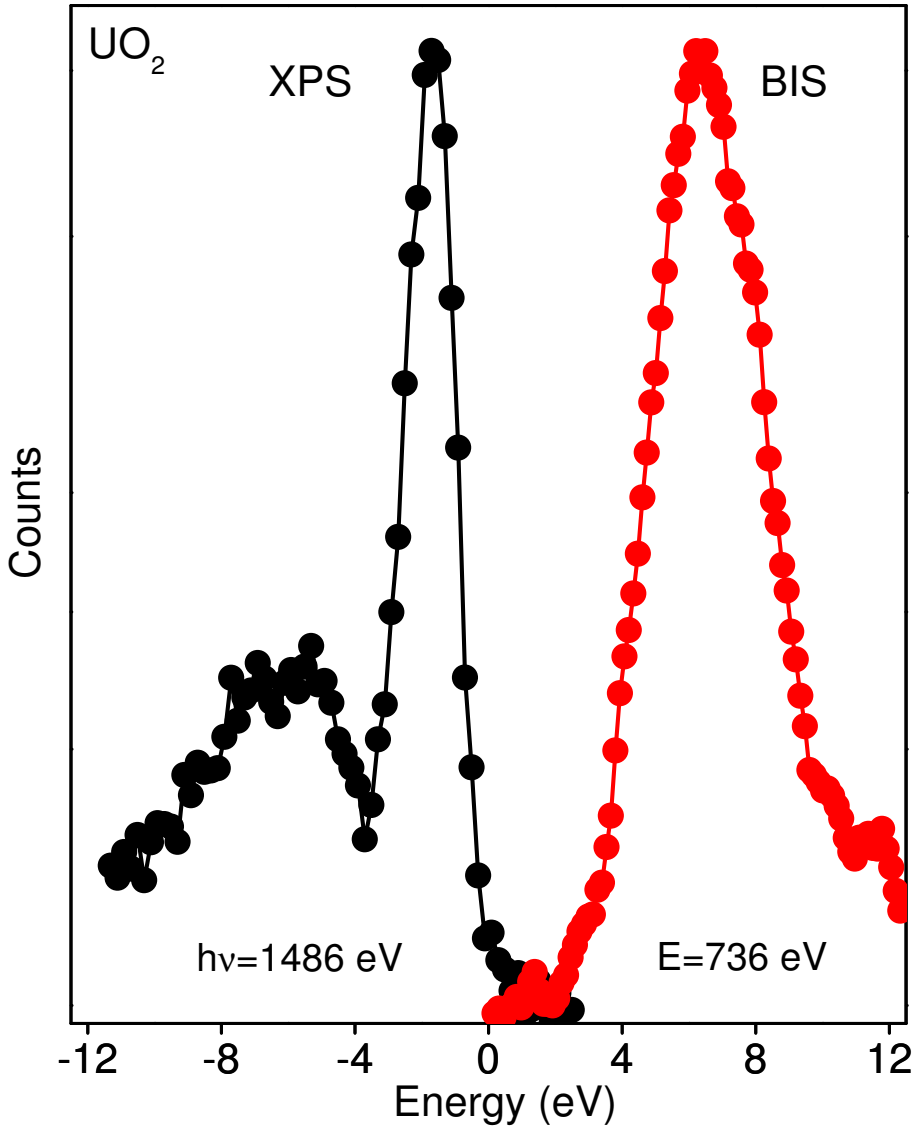

FIG. 8: (Color online) Combination of XPS with hν=1486 eV and BIS with E=736 eV from UO_2.

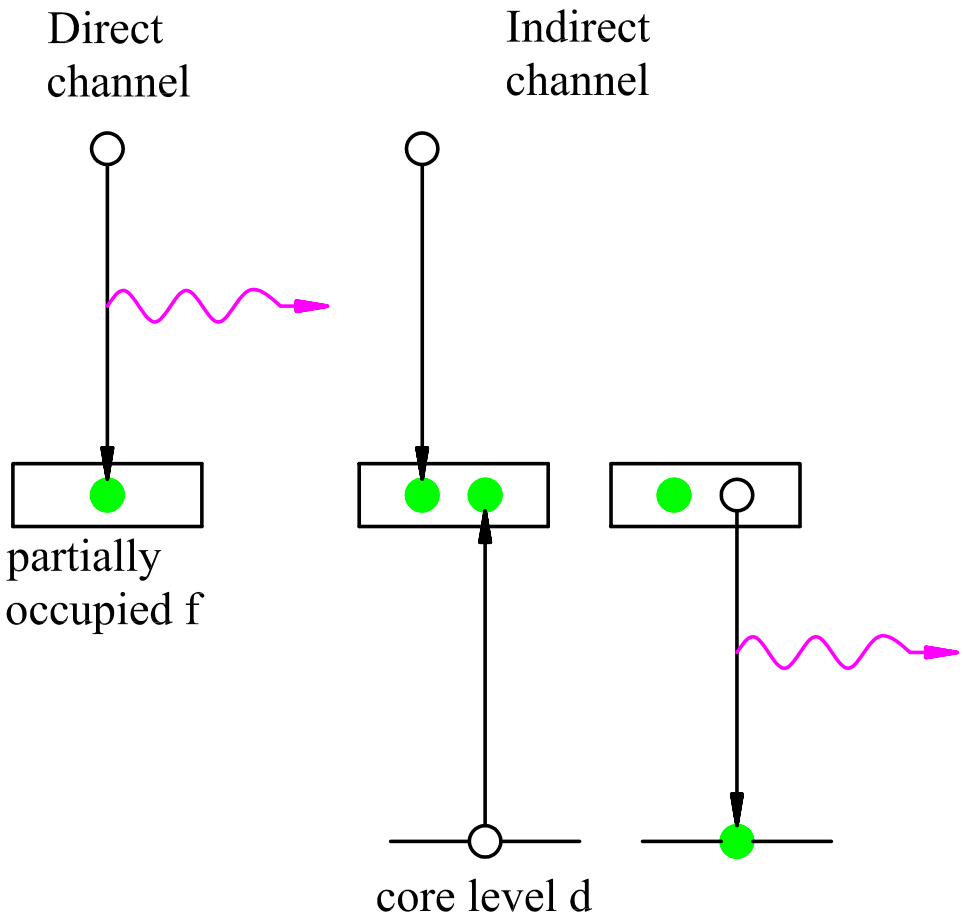

FIG. 9: (Color online) Sketch for resonance inverse photoelectron spectroscopy (RIPES).

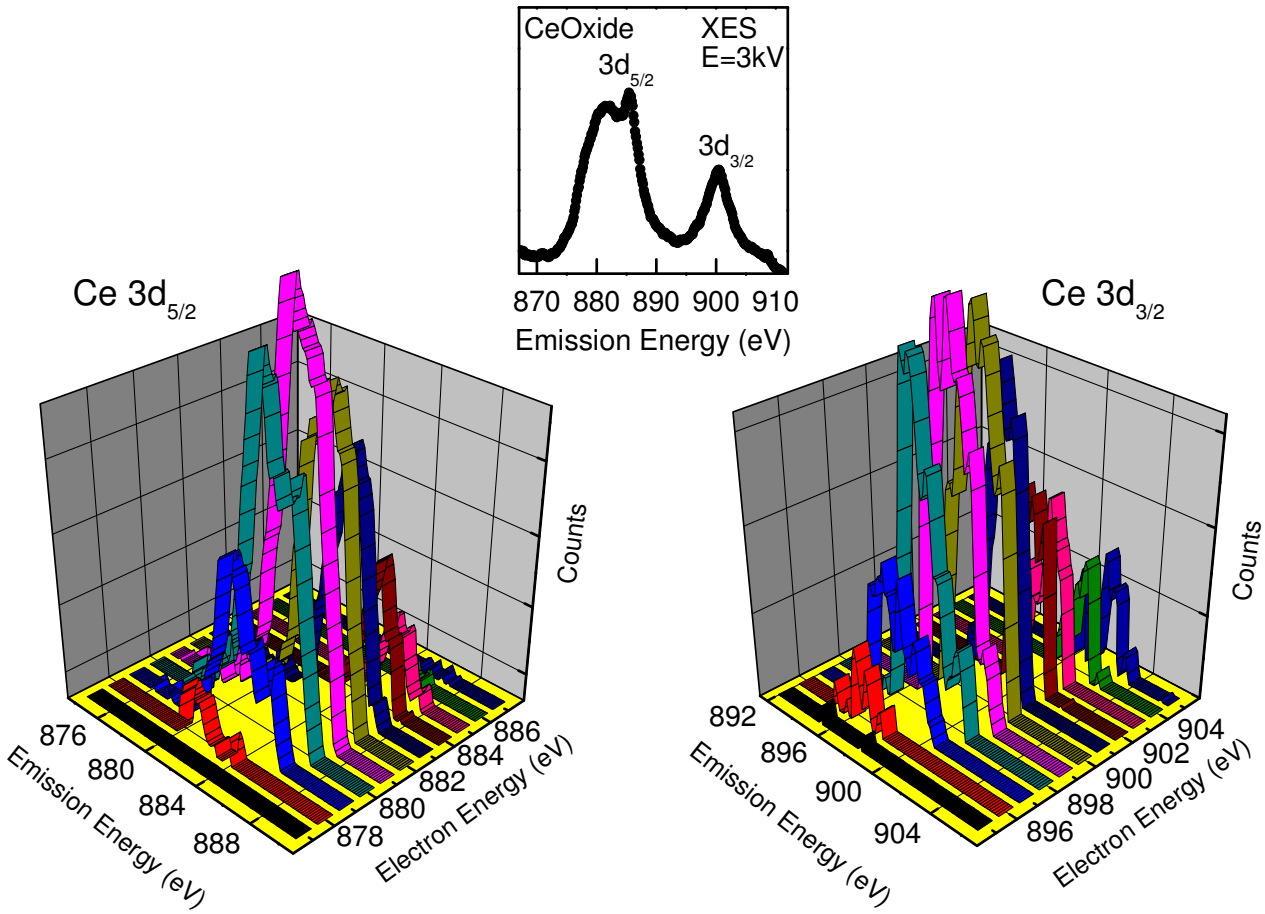

FIG. 10: (Color online) RIPES spectra at Ce $3d_{5/2}$ and $3d_{3/2}$ from Cerium-oxide. XES from Ce 3d with an electron energy of E=3 keV is shown in the middle.